

## Phase diagram of the Bose-Hubbard model on a ring-shaped lattice with tunable weak links

Kalani Hettiarachchilage,<sup>1</sup> Valéry G. Rousseau,<sup>1</sup> Ka-Ming Tam,<sup>1,2</sup> Mark Jarrell,<sup>1,2</sup> and Juana Moreno<sup>1,2</sup>

<sup>1</sup>*Department of Physics and Astronomy, Louisiana State University, Baton Rouge, Louisiana 70803, USA*

<sup>2</sup>*Center for Computation and Technology, Louisiana State University, Baton Rouge, Louisiana 70803, USA*

(Received 21 October 2012; published 24 May 2013)

Motivated by recent experiments on toroidal Bose-Einstein condensates in all-optical traps with tunable weak links, we study the one-dimensional Bose-Hubbard model on a ring-shaped lattice with a small region of weak hopping integrals using quantum Monte Carlo simulations. Besides the usual Mott insulating and superfluid phases, we find a phase which is compressible but nonsuperfluid with a local Mott region. This “local Mott” phase extends in a large region of the phase diagram. These results suggest that the insulating and conducting phases can be tuned by a local parameter, which may provide additional insight into the design of atomtronic devices.

DOI: [10.1103/PhysRevA.87.051607](https://doi.org/10.1103/PhysRevA.87.051607)

PACS number(s): 67.85.Hj, 02.70.Uu, 03.75.Lm, 05.30.Jp

*Introduction.* Cold atom experiments utilizing an optical lattice provide an excellent test bed for quantum many-body problems which were previously inaccessible in conventional materials. A remarkable achievement is the realization of the Bose-Hubbard (BH) model using ultracold atoms on optical lattices [1,2] with the addition of a confining potential that results in the “wedding cake” structure [3]. Over the past two decades, a considerable amount of work has been devoted to understanding the ground-state phase diagram of the BH model and its variants [4–9]. In general, the model contains a superfluid (SF) phase at incommensurate fillings and a Mott insulating (MI) phase at commensurate fillings and strong coupling. The SF phase is gapless, whereas the MI phase is characterized by the existence of an energy gap for creating a particle-hole pair. As the density is changed or the interaction strength is varied, the BH model can be tuned from the MI to the SF. Tuning between insulating and conducting phases by controlling the external parameters provides a tantalizing opportunity of creating analogs to electronic devices and circuits by using ultracold atoms in optical lattices, which have been recently defined as “atomtronics” [10,11]. The conventional electronic system is based on the electron charge, whereas the atomtronic system can use neutral atoms which are either bosons or fermions; moreover, the optical lattice is better controlled. Based on this unique property, it has been suggested that these atomtronic systems may be useful in quantum computing [12]. Some models have already been proposed for atomtronic devices such as batteries, wires, diodes, and transistors [12–20].

A recent advance in optical lattices is the realization of confining potentials with toroidal shapes using the intersection of two different red-detuned laser beams [10,21]. The versatility of this technique allows the creation of ring-shaped lattices by superimposing an optical lattice on a toroidal confining potential, which is a realization of a quasi-one-dimensional lattice with periodic boundary conditions. Remarkably, it is possible to control the local hopping parameter in a region of the ring by applying a magnetic field and an additional laser beam [21]. This opens up the possibility that the different phases in a boson system can be tuned not only by a global parameter, such as the coupling strength or chemical potential, but also by a local parameter, such as the tunneling strength of a small region of the entire lattice. It has been suggested

that this property can be utilized as an alternative realization of atomtronics [21].

In this letter, by using quantum Monte Carlo (QMC), we show that introducing weak links in a ring lattice can produce a local Mott (LM) phase in addition to the usual MI and SF phases present in the homogeneous BH model. Zero-temperature local incompressible MI behavior was shown in a one-dimensional system of interacting bosons in a confining potential [3]. Our nonconfined model exhibits a LM phase which is gapless and non-SF in addition to a region of LM insulator which exhibits incompressible MI behavior. This is an important result which suggests that by controlling the local tunneling strength the system can be tuned between a SF phase and a MI phase through a non-SF LM phase. This provides theoretical support to the idea that atomtronic switches can be implemented by tuning certain local parameters in a quasi-one-dimensional system.

*Model and method.* We consider a bosonic system on a torus-shaped lattice, where the section of the torus is sufficiently small compared to the primary radius so the physics can be reduced to a one-dimensional lattice with periodic boundary conditions. The Hamiltonian takes the form

$$\hat{\mathcal{H}} = -t \sum_{\langle i,j \rangle} w_{ij} (a_i^\dagger a_j + \text{H.c.}) + \frac{U}{2} \sum_{i=1}^L \hat{n}_i (\hat{n}_i - 1), \quad (1)$$

where  $L$  is the number of lattice sites. The creation and annihilation operators  $a_i^\dagger$  and  $a_i$  satisfy bosonic commutation rules,  $[a_i, a_j] = [a_i^\dagger, a_j^\dagger] = 0$ ,  $[a_i, a_j^\dagger] = \delta_{ij}$ , and  $\hat{n}_i = a_i^\dagger a_i$  is the operator that measures the number of bosons on site  $i$ . The parameter  $t$  is the global magnitude of the hopping integral. In this paper, we use  $t = 1$  to set the energy scale. The sum  $\sum_{\langle i,j \rangle}$  runs over all distinct pairs of first neighboring sites  $i$  and  $j$ , and  $w_{ij} \in [0, 1]$  determines the weakness of the hopping integral between  $i$  and  $j$ . In the following we consider a system with  $M$  consecutive weak links for which  $w_{ij} = J/t$ , where  $J \in [0, t]$  is a control parameter, and  $L - M$  strong links with  $w_{ij} = 1$ . We restrict our study to the case with 10% of weak links ( $M = L/10$ ). The parameter  $U$  determines the strength of the on-site interaction.

In order to solve this model, we perform exact QMC in both canonical and grand-canonical ensembles by using the Stochastic Green Function algorithm [22,23] with global

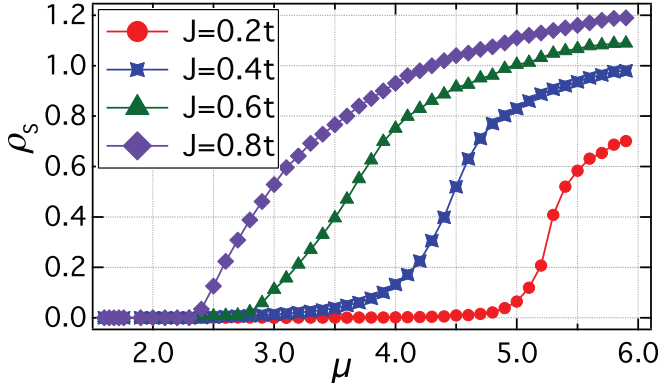


FIG. 1. (Color online) The superfluid density  $\rho_s$  as a function of the chemical potential  $\mu$  for  $L = 50$  and  $U = 8$  in the ground state. The figure shows results for different values of the weak hopping integrals,  $J = 0.2t$  (circles),  $J = 0.4t$  (stars),  $J = 0.6t$  (triangles), and  $J = 0.8t$  (diamond).

space-time updates [24]. In the canonical ensemble, the number of particles  $N$  is a parameter and remains constant during the simulation. The chemical potential  $\mu$  is measured at zero temperature by the finite-energy difference  $\mu(N) = E(N + 1) - E(N)$ . In the grand-canonical ensemble, the number of particles is given by the quantum average of the operator  $\hat{N} = \sum_i \hat{n}_i$  and is controlled by adding to the Hamiltonian (1) the term  $-\mu\hat{N}$  where  $\mu$  is a control parameter. We use an inverse temperature  $\beta = L/t$  in order to capture the ground-state properties.

*Superfluid density and compressibility.* For the uniform system,  $J = t$ , only two phases are present: Mott insulator (MI) and superfluid (SF). The MI phase occurs at commensurate fillings and large onsite repulsion  $U$  and is characterized by a vanishing compressibility,  $\kappa = \frac{\partial \rho}{\partial \mu}$ , where  $\rho = N/L$ . The SF phase is detected by measuring the superfluid density,  $\rho_s$ , given by the response of the system to a phase twist of the wave function at the boundaries. In our QMC simulations, it is convenient to relate this superfluid density to the fluctuations of the winding number,  $W$ , via Pollock and Ceperley's formula [25],  $\rho_s = \frac{\langle W^2 \rangle L}{2t\beta}$ . We have checked analytically and with exact diagonalization that this formula remains valid for the nonuniform system where  $J < t$ .

In the following, we show that there exists a range of parameters for the nonuniform system for which we observe a vanishing superfluid density and a finite compressibility at incommensurate fillings. Figure 1 shows the superfluid density  $\rho_s$  as a function of the chemical potential  $\mu$  for  $L = 50$  and  $U = 8$ . Here we use grand-canonical simulations for different weak link hopping  $J$ . We can clearly see that the region with vanishing superfluid density expands over a large range of chemical potentials  $\mu$  when the strength of the weak links is lowered.

Figure 2 shows the density  $\rho$  and the superfluid density  $\rho_s$  as functions of the chemical potential  $\mu$ , for both homogeneous ( $J = t$ ) and inhomogeneous ( $J = 0.2t$ ) systems, for  $L = 50$  and  $U = 20$ . We can see that a Mott plateau at  $\rho = 1$  exists until  $\mu = 16.1$  with a vanishing superfluid density  $\rho_s$  and compressibility  $\kappa$ , for both systems. For  $\mu > 16.1$ , the density  $\rho$  starts to increase and the compressibility  $\kappa$  is finite. As is well

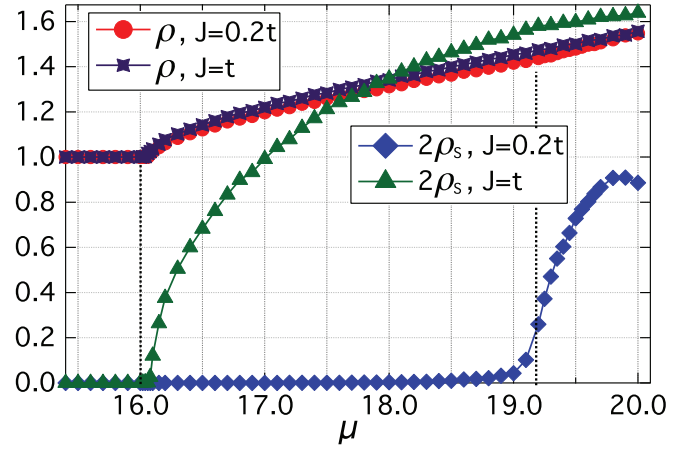


FIG. 2. (Color online) The density  $\rho$  and the superfluid density  $\rho_s$  as functions of the chemical potential  $\mu$  for the homogeneous system ( $J = t$ ) and an inhomogeneous system ( $J = 0.2t$ ), for  $L = 50$  and  $U = 20$ .

known, the superfluid density  $\rho_s$  of the homogeneous system is nonzero as soon as the density is no longer an integer. However, for the inhomogeneous system, the superfluid density remains zero until  $\mu \approx 19.1$ . Thus there exists a finite range of values for the chemical potential for which the superfluid density is vanishing but the compressibility is finite. Therefore, as the chemical potential is increased, the inhomogeneous system undergoes a phase transition from a MI phase to a new phase and then to a SF phase.

*Properties of the phases.* We investigate the intermediate phase first by analyzing the local density of the lattice. The local density in the homogeneous model is uniform, whether the system is in the MI or SF phase. For the inhomogeneous model, we have phases with a nonuniform local density, as shown in Fig. 3(a). We insert 10% of the weak links in the middle of the lattice. In the MI region, the local density  $n_i$  throughout the entire lattice is uniform and sticks to integer values ( $n_i = 1$  for the first Mott lobe,  $n_i = 2$  for the second one, etc).

When additional particles or holes are added to the lattice the weak link region keeps its integer density [see Fig. 3(a)]. Outside the weak link region, the local density shows an oscillatory behavior. Although, based on numerical data, it is difficult to strictly rule out the possibility that the superfluid density is exceedingly small but nonzero in the weak link region, these two observations indicate that the additional particles do not affect the MI character of the weak link until the number of additional particles or holes is beyond a critical density. For a one-dimensional system, the superfluid density or the winding is zero when part of the system is locally Mott. As a result we identify this locally integer-density region as a local Mott (LM) phase. The weak link provides an effective fixed boundary condition for the density profile, and the additional particles or holes accumulate outside. Then, the region with  $J = t$  can be effectively described by the hard-core boson model with  $L - L_{\text{weak}}$  number of sites. For a one-dimensional system, the hard-core boson can be written in terms of spinless fermions using the Jordan-Wigner transformation [26], and the oscillation of the local density

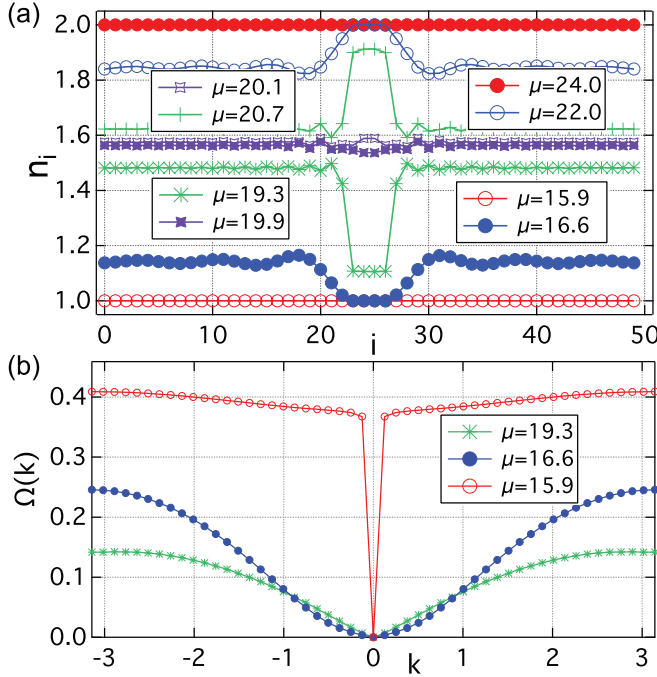


FIG. 3. (Color online) The local density (top panel) and the excitation spectrum (bottom panel) for  $L = 50$  and  $U = 20$ , in the ground state. Top panel: The local density  $n_i$  as a function of the site index  $i$  for different values of the chemical potential  $\mu$ . Bottom panel: The low-energy excitation spectrum  $\Omega(k)$  in the three regions of the phase diagram: SF, LM, and MI.

can then be explained by Friedel oscillations [27], where  $n_i \sim \cos(k_F x_i)$ , where  $k_F$  is the Fermi wave vector given by the particle density. This explanation is corroborated by the numerical data, which show that the cycle of the oscillation of the local density is approximately given by  $1/|n - 1.0|$  for  $\mu = 16.6$  and  $1/|n - 2.0|$  for  $\mu = 22$  [see Fig. 3(a)].

When adding more particles beyond the critical density, the local density at the weak link shifts away from integer values. This suggests that the LM insulating region is destroyed. Thus it opens the path for the flow, and we find that the superfluid density becomes finite when this happens.

We study the dynamics of the model by evaluating the low-energy excitation spectrum. Using the Feynman single-mode approximation, the low-energy excitation spectrum  $\Omega(k)$  can be written as [28]

$$\Omega(k) = \frac{E_k}{S(k)}, \quad (2)$$

where

$$E_k = \frac{-t}{L} (\cos k - 1) \langle \Psi_0 | \sum_{i=1}^L (a_i^\dagger a_{i+1} + a_{i+1}^\dagger a_i) | \Psi_0 \rangle, \quad (3)$$

$|\Psi_0\rangle$  is the ground state, and  $S(k)$  is the static structure factor.

Figure 3(b) displays the low-energy excitation spectrum throughout the reciprocal lattice space. In the MI region it shows a gap near the zero wave vector, whereas it has a linear dependence for the SF phase. The linear behavior is expected in the SF region due to the gapless Goldstone mode. In the LM region the low-energy spectrum shows a parabolic behavior, as expected for disordered free particles. Since the LM does

not follow a linear behavior near  $k = 0$ , no signal of superflow exists in the LM region.

*Ground-state phase diagram.* The MI phase is characterized by an integer local density and the existence of a finite gap for single-particle excitations. At zero temperature, the gap can be easily obtained in the canonical ensemble. We define the gap as  $\Delta = \mu_+ - \mu_-$ , where  $\mu_-$  and  $\mu_+$  are the minimum and maximum values of the chemical potential for which the MI phase exists. By definition,  $\mu_+ = E(N + 1) - E(N)$  and  $\mu_- = E(N) - E(N - 1)$ , where  $N$  is the number of particles in the MI phase. The functions  $\mu_-(t, J, U)$  and  $\mu_+(t, J, U)$  determine the boundaries between the MI and LM regions. Since the total density remains unchanged for  $\mu \in [\mu_-; \mu_+]$ , the compressibility  $\kappa$  is vanishing in the MI region.

We determine the phase boundary between the LM and SF regions by using the grand-canonical simulations and scanning over the chemical potential, as in Fig. 2. The critical value  $\mu_c$  of the chemical potential where the superfluid density becomes nonzero depends on the size of the system,  $L$ , and converges to a finite value in the thermodynamic limit. As the size increases, the curve displaying the superfluid density becomes sharper and sharper. Since we work with a fixed large size,  $L = 50$ , we define  $\mu_c$  by the value of the chemical potential that corresponds to the maximum slope for the superfluid density curve. The curve  $\mu_c(t, J, U)$  determines the boundary between the LM and SF phases.

In our simulations the density varies continuously as a function of the chemical potential. This suggests that the transitions from MI to LM and from LM to SF are continuous, as is the case for the homogeneous model [29–31]. We show in Fig. 4 the ground-state phase diagram for  $J = 0.2t$  in the  $(\mu/U, t/U)$  plane. The Mott lobes that are present in the homogeneous model are weakly deformed by the presence of the LM phase. The phase boundaries near the tip of the Mott lobes are difficult to estimate due to the very small LM region.

We now investigate the variation of the phase boundary between the LM and SF regions as a function of weak link hopping  $J$ , Fig. 5. For a fixed value of the interaction  $U$ , the phase boundary lifts up linearly when decreasing the hopping

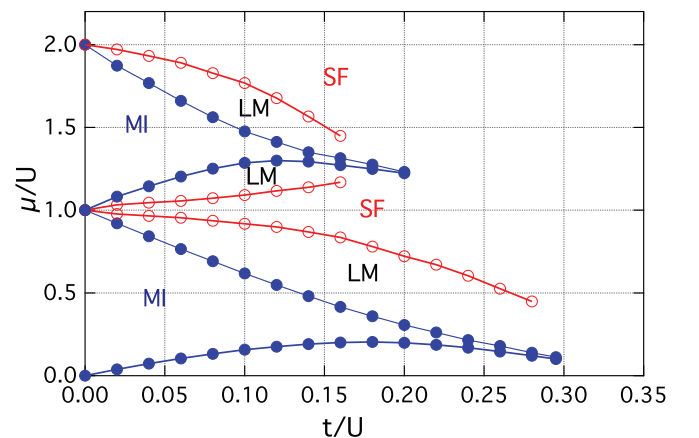


FIG. 4. (Color online) The ground-state phase diagram of the inhomogeneous system ( $J = 0.2t$ ) in the  $(\mu/U, t/U)$  plane. The lines with solid circles show the first and the second Mott lobes, and the lines with open circles show the boundaries between the LM and the SF regions.

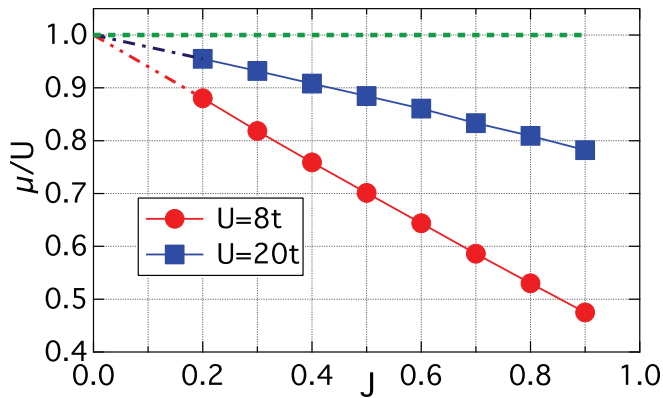


FIG. 5. (Color online) The critical value of the chemical potential  $\mu_c$  between the LM and SF regions, as a function of the weak link hopping  $J$ , for  $U = 8$  and  $U = 20$ . The variation with  $J$  is quasilinear.

$J$  in the weak link, reducing the size of the SF region in the phase diagram. In the limit  $J = 0$  the curve extrapolates to  $\mu/U = 1$ , and the SF region completely disappears since the system is no longer periodic.

**Conclusion.** In this study, we propose that a superconducting ring with weak links might display a phase which is gapless, compressible, and nonsuperfluid, with local Mott insulating behavior. This phase does not exist in the homogeneous Bose-Hubbard model. We expect that in the thermodynamic limit, the weak link acts effectively as a domain wall which suppresses the superfluid. While a thorough characterization of the phases and the critical properties of

the model will require an analysis of the inhomogeneous Luttinger liquid coupled to a lattice, which is an interesting and challenging topic by itself [32–35], we hope our work motivates further study in this direction. Perhaps the most important aspect of the present study is to understand the mechanism of controlling superfluid flow by local perturbation on a finite-size system, which is directly related to atomtronic. In the experiment by Raman *et al.*, a toroidal condensate is created with a smooth trapping potential [21]. If the experiment can be repeated by superimposing a lattice on top of the toroidal potential, our model could be directly studied experimentally. Our results have direct implications for atomtronic devices [12,17]. For example, if the chemical potential  $\mu$ , the weak link hopping  $J$ , and the interaction  $U/t$  are tuned so that only the link is a Mott insulator, then a gate above the link can be used to switch the conductivity of the link on and off. The nonlinearity of the switching can be tuned by adjusting the link width and hopping  $J/t$ . Complex circuits with highly nonlinear behavior may be constructed by a series of such switches.

**Acknowledgments.** We acknowledge Daniel Sheehy for suggesting this problem to us and we thank him and K. C. Wright for useful discussions. This work is supported by NSF OISE-0952300 (K.H., V.G.R., and J.M.) and by DOE SciDAC Grant No. DE-FC02-06ER25792 (K.M.T. and M.J.). This work used the Extreme Science and Engineering Discovery Environment (XSEDE), which is supported by the National Science Foundation Grant No. DMR100007, and the high-performance computational resources provided by the Louisiana Optical Network Initiative.

- 
- [1] D. Jaksch *et al.*, *Phys. Rev. Lett.* **81**, 3108 (1998).  
 [2] M. Greiner *et al.*, *Nature (London)* **415**, 39 (2002).  
 [3] G. G. Batrouni *et al.*, *Phys. Rev. Lett.* **89**, 117203 (2002).  
 [4] M. P. A. Fisher *et al.*, *Phys. Rev. B* **40**, 546 (1989).  
 [5] G. G. Batrouni *et al.*, *Phys. Rev. Lett.* **65**, 1765 (1990).  
 [6] W. Krauth and N. Trivedi, *Europhys. Lett.* **14**, 627 (1991).  
 [7] M. C. Cha *et al.*, *Phys. Rev. B* **44**, 6883 (1991).  
 [8] J. K. Freericks and H. Monien, *Phys. Rev. B* **53**, 2691 (1996).  
 [9] A. Nunnenkamp *et al.*, *Phys. Rev. A* **77**, 023622 (2008).  
 [10] C. Ryu *et al.*, *Phys. Rev. Lett.* **99**, 260401 (2007).  
 [11] S. G. Bhongale *et al.*, *Phys. Rev. Lett.* **108**, 145301 (2012).  
 [12] R. A. Pepino *et al.*, *Phys. Rev. Lett.* **103**, 140405 (2009).  
 [13] A. Ruschhaupt and J. G. Muga, *Phys. Rev. A* **70**, 061604(R) (2004).  
 [14] A. Ruschhaupt and J. G. Muga, *Phys. Rev. A* **73**, 013608 (2006).  
 [15] A. Ruschhaupt and J. G. Muga, *J. Phys. B: At. Mol. Opt. Phys.* **41**, 205503 (2008).  
 [16] C. P. Rubbo *et al.*, *Phys. Rev. A* **84**, 033638 (2011).  
 [17] B. T. Seaman *et al.*, *Phys. Rev. A* **75**, 023615 (2007); V. G. Rousseau *et al.*, *Phys. Rev. B* **72**, 054524 (2005).  
 [18] J. A. Stickney *et al.*, *Phys. Rev. A* **75**, 013608 (2007).  
 [19] A. Micheli *et al.*, *Phys. Rev. Lett.* **93**, 140408 (2004).  
 [20] J. Y. Vaishnav *et al.*, *Phys. Rev. Lett.* **101**, 265302 (2008).  
 [21] A. Ramanathan *et al.*, *Phys. Rev. Lett.* **106**, 130401 (2011).  
 [22] V. G. Rousseau, *Phys. Rev. E* **77**, 056705 (2008).  
 [23] V. G. Rousseau, *Phys. Rev. E* **78**, 056707 (2008).  
 [24] V. G. Rousseau and D. Galanakis, arXiv:1209.0946.  
 [25] E. L. Pollock and D. M. Ceperley, *Phys. Rev. B* **36**, 8343 (1987).  
 [26] P. Jordan and E. Wigner, *Z. Phys.* **47**, 631 (1928).  
 [27] J. Friedel, *Nuovo Cimento Suppl.* **7**, 287 (1958).  
 [28] R. T. Scalettar *et al.*, *J. Low Temp. Phys.* **140**, 313 (2005).  
 [29] T. D. Kuhner *et al.*, *Phys. Rev. B* **61**, 12474 (1999).  
 [30] V. A. Kashurnikov *et al.*, *JETP Lett.* **64**, 99 (1996).  
 [31] V. F. Elesin *et al.*, *JETP Lett.* **60**, 177 (1994).  
 [32] J. Rech and K. A. Matveev, *J. Phys.: Condens. Matter* **20**, 164211 (2008).  
 [33] D. L. Maslov and M. Stone, *Phys. Rev. B* **52**, R5539 (1995).  
 [34] I. Safi and H. J. Schulz, *Phys. Rev. B* **52**, R17040 (1995).  
 [35] V. V. Ponomarenko, *Phys. Rev. B* **52**, R8666 (1995).